Journal of the Korean Society for Noise and Vibration Engineering, Vol. 4, No. 4, pp. 435～442, 1994.

〈**Original**〉

An Investigation of Dynamic Stability of Self-Compensating Dynamic Balancer

자기보상 동적균형기의 동적안정성 연구

Jongkil Lee*

이 종 길

〈Received June 3, 1994 ; Accepted October 12, 1994〉

ABSTRACT

Self-Compensating Dynamic Balancer (SCDB) is composed of a circular disk with a groove containing spherical balls and a low viscosity damping fluid. To investigate the stability of the motion equations these equations are perturbed and the resulting perturbation equations are analyzed further to determine whether the perturbations grow or decay with dimensionless time. Based on the results of stability investigation, ball positions that result in a balanced system are stable above the critical speed for $\beta'=3.8$. At critical speed the perturbed motion is said to be stable for $\beta'=23$. However, the system is unstable below critical speed in any case of β'.

요 약

자기보상 동적균형기는 홈이파인 원형판에 강구와 저점성유체를 지닌 구조체이다. 유도된 운동방정식의 안정성을 조사하기 위하여 섭동이론을 통하여 무차원화한 시간에 따라 섭동방정식의 특성을 조사하였다. 안정성연구의 결과에 근거하여 임계속도보다 높은 범위에서 β'이 3.8 이상이면 자기보상 동적균형기는 정상작동을 보여주었다. 임계속도에서는 β'이 23이면 정상작동(안정성)을 하였으나 임계속도보다 낮은 범위에서는 어떠한 β'에 대해서도 불안정함을 알 수 있었다.

1. Introduction

The unbalance in the rotors of rotating machinery causes rotor vibrations and generates undesirable forces. For simple rotors the correction procedure is carried out by adding one or more balance weights to the rotor at the correct angular orientation. However, in the case of long flexible rotors the correction procedure is more complicated. Instead of using a dynamic balancing machine, the Self-Compensating Dynamic Balancer (SCDB), or automatic dynamic balancer, has been proposed in many patents to minimize the effects of rotor unbalance and vibratory forces on the rotating system during normal operation. The SCDB is usually composed of a circular disk with a groove or race containing spherical balls or cylindrical rollers and a low viscosity damping fluid, although early attempts used other approaches. The concept is applicable in many fields such as space vehicle components, commercial machines which have rotating shafts, automobile wheels, etc. However, the investigators left it for others to explain why this system will work. Therefore, the objective of this research is to investigate the dynamic stability of SCDB.

*Member, Hyundai Heavy Industries Co., Ltd., Noise and Vibration Research Department

2. Nondimensional Equations of Motion

A rotating shaft with SCDB carrying an unbalance disk at its midspan is shown in Figure 1. The side view of a general position of the rotating disk of mass M and the balls, each of mass m, is shown in Figure 2. The point C represents the deflected centerline of the rotating system, and the point G represents the location of the mass center of the disk and SCDB. Assuming that the center C of the disk is located at the origin O of the XYZ axes when the shaft is aligned between the bearings, the lateral deflection of the shaft at the location of the disk is OC.

The equations of motion of the system can be

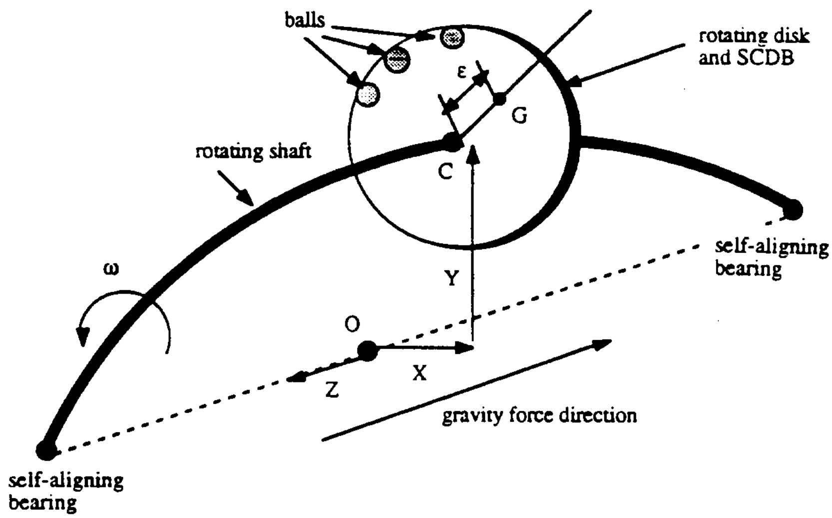

Fig. 1 Rotating system of the SCDB

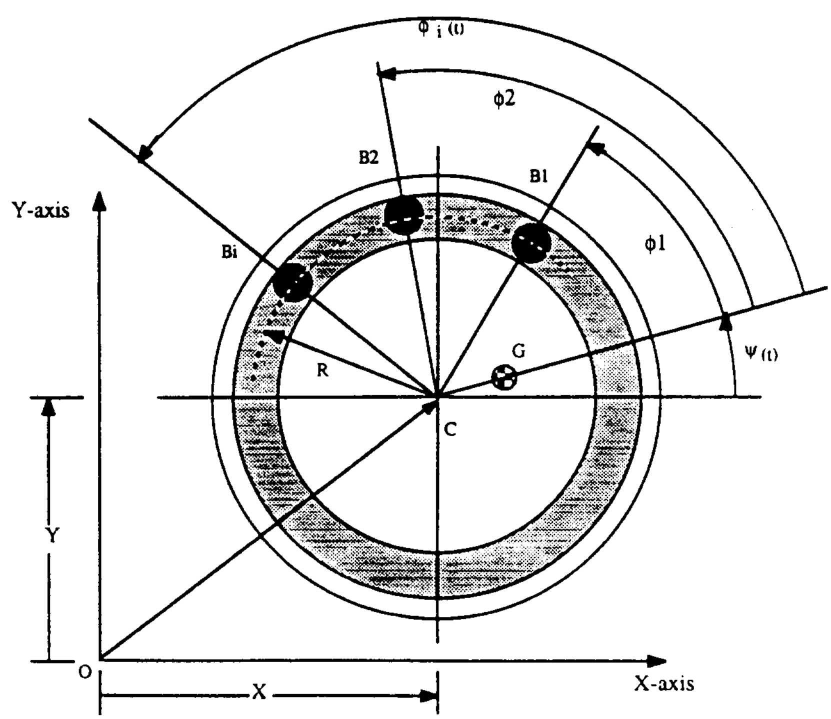

Fig. 2 Self-compensating dynamic balancer

derived by the Lagrangian method. For a circular shaft it is logical to assume that the stiffness, k, and the damping of the shaft, c, are the same regardless of the orientation of the shaft. It is assumed that the balls slide along the race because of drag force in fluid. Therefore, a scalar Lagrangian function, L, is

$$L=\frac{1}{2}I_Z\dot{\Psi}^2+\frac{1}{2}M[\dot{X}^2+\dot{Y}^2-2\varepsilon\dot{\Psi}\dot{X}\sin\Psi+\varepsilon^2\dot{\Psi}^2+2\varepsilon\dot{\Psi}\dot{Y}\cos\Psi]+\frac{1}{2}\sum_{i=1}^{n}\left(m_i+\frac{2}{5}m_i\right)\{\dot{X}^2+\dot{Y}^2+(\dot{\phi}_i+\dot{\Psi})^2R^2-2R(\dot{\phi}_i+\dot{\Psi})[\dot{X}\sin(\phi_i+\Psi)-\dot{Y}\cos(\phi_i+\Psi)]\}-\frac{1}{2}k(X^2+Y^2) \quad (1)$$

where, gravitational effects have been ignored. I_Z is mass moment of inertia of the disk. If the angular velocity of the disk is constant, then $\ddot{\Psi}=0$, $\dot{\Psi}=\omega$ and $\Psi=\omega t$ where, ω is a rotation speed of the shaft. In this case equations of motion are obtained by

$$\left[1+n\left(\frac{m}{M}\right)\right]\frac{\ddot{X}}{\omega_n^2 R}+\frac{2\zeta}{\omega_n}\frac{\dot{X}}{R}+\frac{X}{R}-\frac{\varepsilon}{R}\left(\frac{\omega}{\omega_n}\right)^2\cos(\omega t)-\frac{1}{\omega_n^2}\frac{m}{M}\sum_{i=1}^{n}[\ddot{\phi}_i\sin(\phi_i+\omega t)+(\dot{\phi}_i+\omega)^2\cos(\phi_i+\omega t)]=0, \quad (2)$$

$$\left[1+n\left(\frac{m}{M}\right)\right]\frac{\ddot{Y}}{\omega_n^2 R}+\frac{2\zeta}{\omega_n}\frac{\dot{Y}}{R}+\frac{Y}{R}-\frac{\varepsilon}{R}\left(\frac{\omega}{\omega_n}\right)^2\sin(\omega t)+\frac{1}{\omega_n^2}\frac{m}{M}\sum_{i=1}^{n}[\ddot{\phi}_i\cos(\phi_i+\omega t)-(\dot{\phi}_i+\omega)^2\sin(\phi_i+\omega t)]=0, \quad (3)$$

$$\frac{\ddot{\phi}_i}{\omega_n^2}-\frac{1}{\omega_n^2}\frac{\ddot{X}}{R}\sin(\phi_i+\omega t)+\frac{1}{\omega^{n2}}\frac{\ddot{Y}}{R}\cos(\phi_i+\omega t)+\frac{1}{R\omega_n^2}(\dot{\phi}_i+\omega)[\dot{X}\cos(\phi_i+\omega t)+\dot{Y}\sin(\phi_i+\omega t)]=-\beta\frac{\dot{\phi}_i}{\omega_n^2}(\text{for } i=1,\ 2,\ \cdots,\ n), \quad (4)$$

where,

$$\frac{m}{M}=\frac{m_i+\frac{2}{5}m_i}{M} \text{ and } \beta=\frac{D}{\left(m_i+\frac{2}{5}m_i\right)R^2} \quad (\text{for } i=1,\ 2,\ \cdots,\ n). \quad (5)$$

D is drag force per unit angular velocity and n is number of the balls. The natural circular frequency of the rotating system, ω_n, and the damping factor, ζ, are given by $\omega_n=\sqrt{\frac{k}{M}}$ and $\zeta=\frac{c}{2\sqrt{kM}}$, respectively. To get nondimensional equations of motion, introduce

$$t=\omega_n^{-1}\bar{t},\quad X=R\tilde{x},\text{ and } Y=R\tilde{y}, \quad (6)$$

where X, Y, and t are dimensional displacements and time and $\tilde{x}$, $\tilde{y}$, and $\bar{t}$, are nondimensional displacements and time, respectively. Substituting Eq. (6) into the Eqs. (2), (3), and (4) then gives

$$\left[1+n\left(\frac{m}{M}\right)\right]\ddot{\tilde{x}}+2\zeta\dot{\tilde{x}}+\tilde{x}-\frac{\varepsilon}{R}\left(\frac{\omega}{\omega_n}\right)^2\cos\left(\frac{\omega}{\omega_n}\bar{t}\right)-\frac{m}{M}\sum_{i=1}^{n}\left[\ddot{\phi}_i\sin\left(\phi_i+\frac{\omega}{\omega_n}\bar{t}\right)+\left(\dot{\phi}_i+\frac{\omega}{\omega_n}\right)^2\cos\left(\phi_i+\frac{\omega}{\omega_n}\bar{t}\right)\right]=0, \quad (7)$$

$$\left[1+n\left(\frac{m}{M}\right)\right]\ddot{\tilde{y}}+2\zeta\dot{\tilde{y}}+\tilde{y}-\frac{\varepsilon}{R}\left(\frac{\omega}{\omega_n}\right)^2\sin\left(\frac{\omega}{\omega_n}\bar{t}\right)+\frac{m}{M}\sum_{i=1}^{n}\left[\ddot{\phi}_i\cos\left(\phi_i+\frac{\omega}{\omega_n}\bar{t}\right)-\left(\dot{\phi}_i+\frac{\omega}{\omega_n}\right)^2\sin\left(\phi_i+\frac{\omega}{\omega_n}\bar{t}\right)\right]=0, \quad (8)$$

$$\ddot{\phi}_i-\ddot{\tilde{x}}\sin\left(\phi_i+\frac{\omega}{\omega_n}\bar{t}\right)+\ddot{\tilde{y}}\cos\left(\phi_i+\frac{\omega}{\omega_n}\bar{t}\right)+\left(\dot{\phi}_i+\frac{\omega}{\omega_n}\right)\left[\dot{\tilde{x}}\cos\left(\phi_i+\frac{\omega}{\omega_n}\bar{t}\right)+\dot{\tilde{y}}\sin\left(\phi_i+\frac{\omega}{\omega_n}\bar{t}\right)\right]=-\beta'\dot{\phi}_i \quad (9)$$

where,

$$\beta'=\frac{\beta}{\omega_n}=\frac{D}{\left(m_i+\frac{2}{5}m_i\right)R^2\omega_n} \quad (10)$$

3. Steady Solution

We will seek solutions where X and Y are zero and the balls have reached an equilibrium position. This is clearly the desired operating condition for the SCDB. When the balls are located at the equilibrium position, then

$$X=\dot{X}=\ddot{X}=0,\quad Y=\dot{Y}=\ddot{Y}=0 \quad\text{and}\quad \dot{\phi}_i=\ddot{\phi}_i=0. \quad (11)$$

In this case Eqs. (2) and (3) can be expressed as

$$\frac{\varepsilon}{R}\cos(\omega t)+\frac{m}{M}\sum_{i=1}^{n}[\cos\phi_i\cos(\omega t)-\sin\phi_i\sin(\omega t)]=0 \quad (12)$$

$$\frac{\varepsilon}{R}\sin(\omega t)+\frac{m}{M}\sum_{i=1}^{n}[\sin\phi_i\cos(\omega t)+\cos\phi_i\sin(\omega t)]=0, \quad (13)$$

respectively. Multiplying (12) by $\cos(\omega t)$ and (13) by

$\sin(\omega t)$, then adding the resulting equations, gives

$$\frac{\varepsilon}{R}+\frac{m}{M}\sum_{i=1}^{n}\cos\phi_i=0. \tag{14}$$

Multiplying (12) by $\sin(\omega t)$ and (13) by $\cos(\omega t)$, then subtracting the resulting equations gives

$$\sum_{i=1}^{n}\sin\phi_i=0. \tag{15}$$

Equations (14) and (15) must both be satisfied for the rotating system to be in a state of balance. According to the Eqs. (14) and (15), a rotating system is said to be in a state of balance when the resultant of all centrifugal forces acting on the rotating system is zero and the centrifugal forces do not give rise to any couple acting on the rotating system.

4. Perturbation Equations

To investigate the stability of the motion equations, these equations are first perturbed and the resulting equations are analyzed further to determine whether the perturbations grow or decay with time. According to this techniques, the solution is represented by the first few terms of an asymptotic expansion, usually not more than two terms. Suppose that the balls have some slight displacements from dynamic equilibrium positions, ϕ_{si} which are constants. Let

$$\phi_i=\phi_{si}+\varepsilon\phi_i+O(\varepsilon^2),\quad (\text{for } i=1,\ 2,\ \cdots,\ n) \tag{16}$$

$$\tilde{x}=\tilde{x}_o+\varepsilon\tilde{x}_1+O(\varepsilon^2), \tag{17}$$

$$\tilde{y}=\tilde{y}_o+\varepsilon\tilde{y}_1+O(\varepsilon^2), \tag{18}$$

We seek approximate solutions which are uniformly valid for small ε. To simplify the Eqs. (7), (8), and (9), let

$$\frac{\omega}{\omega_n}=\tilde{\omega},\quad \frac{\varepsilon}{R}=\tilde{R},\ \text{and}\ \frac{m}{M}=\tilde{m}. \tag{19}$$

Substituting Eqs. (16), (17), (18), and (19) into the Eqs. (7), (8), and (9) then the nondimensional equations of motion are obtained as

$$\begin{aligned}&(1+n\tilde{m})(\ddot{\tilde{x}}_0+\varepsilon\ddot{\tilde{x}}_1)+2\zeta(\dot{\tilde{x}}_0+\varepsilon\dot{\tilde{x}}_1)\\&+(\tilde{x}_0+\varepsilon\tilde{x}_1)-\tilde{R}\tilde{\omega}^2\cos(\tilde{\omega}\tilde{t})\\&-\tilde{m}\sum_{i=1}^{n}\{\varepsilon\ddot{\phi}_i[\sin(\phi_{si}+\tilde{\omega}\tilde{t})\\&+\cos(\phi_{si}+\tilde{\omega}\tilde{t})\varepsilon\phi_i]\\&+[\tilde{\omega}^2+\varepsilon(2\tilde{\omega}\dot{\phi}_i+\varepsilon\dot{\phi}_i^2)][\cos(\phi_{si}+\tilde{\omega}\tilde{t})\\&-\varepsilon\phi_i\sin(\phi_{si}+\tilde{\omega}\tilde{t})]\}+O(\varepsilon^2)=0,\end{aligned} \tag{20}$$

$$\begin{aligned}&(1+n\tilde{m})(\ddot{\tilde{y}}_0+\varepsilon\ddot{\tilde{y}}_1)+2\zeta(\dot{\tilde{y}}_0+\varepsilon\dot{\tilde{y}}_1)\\&+(\tilde{y}_0+\varepsilon\tilde{y}_1)-\tilde{R}\tilde{\omega}^2\sin(\tilde{\omega}\tilde{t})\\&+\tilde{m}\sum_{i=1}^{n}\{\varepsilon\ddot{\phi}_i[\cos(\phi_{si}+\tilde{\omega}\tilde{t})-\varepsilon\phi_i\sin(\phi_{si}\\&+\tilde{\omega}\tilde{t})]-[\tilde{\omega}^2+\varepsilon(2\tilde{\omega}\dot{\phi}_i+\varepsilon\dot{\phi}_i^2)][\sin(\phi_{si}\\&+\tilde{\omega}\tilde{t})+\cos(\phi_{si}+\tilde{\omega}\tilde{t})\varepsilon\phi_i]\}+O(\varepsilon^2)=0,\end{aligned} \tag{21}$$

$$\begin{aligned}&\varepsilon\ddot{\phi}_i-(\ddot{\tilde{x}}_0+\varepsilon\ddot{\tilde{x}}_1)[\sin(\phi_{si}+\tilde{\omega}\tilde{t})+\cos(\phi_{si}\\&+\tilde{\omega}\tilde{t})\varepsilon\phi_i]+(\ddot{\tilde{y}}_0+\varepsilon\ddot{\tilde{y}}_1)[\cos(\phi_{si}+\tilde{\omega}\tilde{t})\\&-\varepsilon\phi_i\sin(\phi_{si}+\tilde{\omega}\tilde{t})]\\&+(\varepsilon\dot{\phi}_i+\tilde{\omega})\{\dot{\tilde{x}}_0+\varepsilon\dot{\tilde{x}}_1)[\cos(\phi_{si}+\tilde{\omega}\tilde{t})-\varepsilon\phi_i\\&\sin(\phi_{si}+\tilde{\omega}\tilde{t})]+(\dot{\tilde{y}}_0+\varepsilon\dot{\tilde{y}}_1)[\sin(\phi_{si}+\tilde{\omega}\tilde{t})\\&+\cos(\phi_{si}+\tilde{\omega}\tilde{t})\varepsilon\phi_i]\}+O(\varepsilon^2)=-\beta'\varepsilon\dot{\phi}_i\end{aligned} \tag{22}$$

Equating the coefficients of power of ε^0 and using the Eqs. (14) and (15) then gives

$$\begin{aligned}&(1+n\tilde{m})\ddot{\tilde{x}}_0+2\zeta\dot{\tilde{x}}_0+\tilde{x}_0=\tilde{R}\tilde{\omega}^2\cos(\tilde{\omega}\tilde{t})\\&+\tilde{m}\sum_{i=1}^{n}\tilde{\omega}^2\cos(\phi_{si}+\tilde{\omega}\tilde{t})\\&=\tilde{\omega}^2[(\tilde{R}+\tilde{m}\sum_{i=1}^{n}\cos\phi_{si})\cos(\tilde{\omega}\tilde{t})-\tilde{m}\sum_{i=1}^{n}\sin\\&\phi_{si}\ \sin(\tilde{\omega}\tilde{t})]=0,\end{aligned} \tag{23}$$

$$\begin{aligned}&(1+n\tilde{m})\ddot{\tilde{y}}_0+2\zeta\dot{\tilde{y}}_0+\tilde{y}_0=\tilde{R}\tilde{\omega}^2\sin(\tilde{\omega}\tilde{t})\\&+\tilde{m}\sum_{i=1}^{n}\tilde{\omega}^2\sin(\phi_{si}+\tilde{\omega}\tilde{t})\\&=\tilde{\omega}^2[(\tilde{R}+\tilde{m}\sum_{i=1}^{n}\cos\phi_{si})\sin(\tilde{\omega}\tilde{t})+\tilde{m}\sum_{i=1}^{n}\sin\\&\phi_{si}\ \cos(\tilde{\omega}\tilde{t})]=0.\end{aligned} \tag{24}$$

These equations are transient oscillations that decay with time. If the shaft is initially disturbed, $\tilde{x}$ and $\tilde{y}$ are not zero but become zero as the oscillations decay. Equating coefficients of like power of ε^1 yields

$$\begin{aligned}&(1+n\tilde{m})\ddot{\tilde{x}}_1+2\zeta\dot{\tilde{x}}_1+\tilde{x}_1=\tilde{m}\sum_{i=1}^{n}\{\ddot{\phi}_i\sin(\phi_{si}+\tilde{\omega}\tilde{t})\\&-\tilde{\omega}^2\phi_i\sin(\phi_{si}+\tilde{\omega}\tilde{t})+2\tilde{\omega}\dot{\phi}_i\cos(\phi_{si}+\tilde{\omega}\tilde{t})\end{aligned} \tag{25}$$

$$\begin{aligned}&(1+n\tilde{m})\ddot{\tilde{y}}_1+2\zeta\dot{\tilde{y}}_1+\tilde{y}_1=-\tilde{m}\sum_{i=1}^{n}\{\ddot{\phi}_i\cos(\phi_{si}\\&+\tilde{\omega}\tilde{t})-\tilde{\omega}^2\phi_i\cos(\phi_{si}+\tilde{\omega}\tilde{t})-2\tilde{\omega}\dot{\phi}_i\sin(\phi_{si}\\&+\tilde{\omega}\tilde{t})\end{aligned} \tag{26}$$

$$\begin{aligned}&\ddot{\phi}_i-\ddot{\tilde{x}}_0\phi_i\cos(\phi_{si}+\tilde{\omega}\tilde{t})-\ddot{\tilde{x}}_1\sin(\phi_{si}+\tilde{\omega}\tilde{t})\\&-\ddot{\tilde{y}}_0\phi_i\sin(\phi_{si}+\tilde{\omega}\tilde{t})+\ddot{\tilde{y}}_1\cos(\phi_{si}+\tilde{\omega}\tilde{t})+\dot{\phi}_i\dot{\tilde{x}}_0\\&\cos(\phi_{si}+\tilde{\omega}\tilde{t})\end{aligned}$$

$$+\dot{\phi}_i\dot{y}_0\sin(\phi_{si}+\tilde{\omega}\bar{t})-\tilde{\omega}\dot{x}_0\phi_i\sin(\phi_{si}+\tilde{\omega}\bar{t})$$
$$+\tilde{\omega}\dot{x}_1\cos(\phi_{si}+\tilde{\omega}\bar{t})+\tilde{\omega}\dot{y}_0\phi_i\cos(\phi_{si}+\tilde{\omega}\bar{t})$$
$$+\tilde{\omega}\dot{y}_1\sin(\phi_{si}+\tilde{\omega}\bar{t})=-\beta'\dot{\phi}_i. \qquad (27)$$

5. Dynamic Stability

The perturbed equations, (25), (26), and (27) do not appear to be able to be integratable in closed form. Therefore, to investigate the stability of the perturbed equations it is convenient to utilize the fact that a system of n second order equations can be transformed into a system of 2n first order equations. Let us introduce six state variables,

$$\{\eta_1\eta_2\eta_3\eta_4\eta_5\eta_6\}^T=\{\tilde{x}_1,\ \dot{\tilde{x}}_1,\ \tilde{y}_1,\ \dot{\tilde{y}}_1,\ \phi_1,\ \dot{\phi}_1\}^T \text{ and}$$
$$\{\dot{\eta}_2\dot{\eta}_4\dot{\eta}_6\}^T=\{\ddot{\tilde{x}}_1\ddot{\tilde{y}}_1\ddot{\phi}_1\}^T. \qquad (28)$$

For convenience, consider only the one ball case. Therefore, using the state-space method, the perturbed equations, (25), (26), and (27), can be expressed by

$$\{\dot{\eta}_1\ \dot{\eta}_2\ \dot{\eta}_3\ \dot{\eta}_4\ \dot{\eta}_5\ \dot{\eta}_6\}^T=[A(\bar{t})]\{\eta_1\eta_2\eta_3\eta_4\eta_5\eta_6\}^T \qquad (29)$$

where, the system matrix, $[A(\bar{t})]$, is defined as

$$[A(\bar{t})]=\begin{bmatrix} 0 & 1 & 0 & 0 & 0 & 0 \\ A_{21} & A_{22} & A_{23} & A_{24} & A_{25} & A_{26} \\ 0 & 0 & 0 & 1 & 0 & 0 \\ A_{41} & A_{42} & A_{43} & A_{44} & A_{45} & A_{46} \\ 0 & 0 & 0 & 0 & 0 & 1 \\ A_{61} & A_{62} & A_{63} & A_{64} & A_{65} & A_{66} \end{bmatrix} \qquad (30)$$

and the elements of the system matrix, $[A(\bar{t})]$, are expressed by

$$A_{21}=-(1+\tilde{m})[1+\tilde{m}\sin^2(\phi_{s1}+\tilde{\omega}\bar{t})]/(1+\tilde{m})^2, \qquad (31)$$

$$A_{22}=[-2\zeta(1+\tilde{m})-2\zeta(1+\tilde{m})\sin^2(\phi_{s1}+\tilde{\omega}\bar{t})$$
$$+\tilde{m}^2(1+\tilde{m})\tilde{\omega}\sin(\phi_{s1}+\tilde{\omega}\bar{t})\cos(\phi_{s1}+\tilde{\omega}\bar{t})$$
$$-\tilde{m}(1+\tilde{m})\tilde{\omega}\sin(\phi_{s1}+\tilde{\omega}\bar{t})\cos(\phi_{s1}+\tilde{\omega}\bar{t})]/$$
$$(1+\tilde{m})^2, \qquad (32)$$

$$A_{23}=\tilde{m}(1+\tilde{m})\sin(\phi_{s1}+\tilde{\omega}\bar{t})\cos(\phi_{s1}+\tilde{\omega}\bar{t})/$$
$$(1+\tilde{m})^2, \qquad (33)$$

$$A_{24}=[2\zeta\tilde{m}(1+\tilde{m})\sin(\phi_{s1}+\tilde{\omega}\bar{t})\cos(\phi_{s1}+\tilde{\omega}\bar{t})$$
$$-\tilde{m}(1+\tilde{m})\tilde{\omega}\sin^2(\phi_{s1}+\tilde{\omega}\bar{t})](1+\tilde{m})^2,$$

$$A_{25}=[-\tilde{m}(1+\tilde{m})\tilde{\omega}^2\sin(\phi_{s1}+\tilde{\omega}\bar{t})-\tilde{m}^2(1+\tilde{m})$$
$$\tilde{\omega}^2\sin(\phi_{s1}+\tilde{\omega}\bar{t})]/(1+\tilde{m})^2, \qquad (34)$$

$$A_{26}=[2\tilde{m}(1+\tilde{m})\tilde{\omega}\cos(\phi_{s1}+\tilde{\omega}\bar{t})-\tilde{m}(1+\tilde{m})^2$$
$$\sin^2(\phi_{s1}+\tilde{\omega}\bar{t})$$
$$-\tilde{m}\mathrm{B}'(1+\tilde{m})^2\sin(\phi_{s1}+\tilde{\omega}\bar{t})]/(1+\tilde{m})^2, \qquad (35)$$

$$A_{41}=-(1+\tilde{m})\tilde{m}\sin(\phi_{s1}+\tilde{\omega}\bar{t})\cos(\phi_{s1}$$
$$+\tilde{\omega}\bar{t})/(1+\tilde{m})^2, \qquad (36)$$

$$A_{42}=[\tilde{m}(1+\tilde{m})\tilde{\omega}\cos^2[\phi_{s1}+\tilde{\omega}\bar{t})+\tilde{m}^2(1+\tilde{m})$$
$$\tilde{\omega}\cos^2(\phi_{s1}+\tilde{\omega}\bar{t})$$
$$-2\tilde{m}(1+\tilde{m})\zeta\sin(\phi_{s1}+\tilde{\omega}\bar{t})\cos(\phi_{s1}+\tilde{\omega}\bar{t})]/$$
$$(1+\tilde{m})^2, \qquad (37)$$

$$A_{43}=-(1+\tilde{m})[1-\tilde{m}\cos^2(\phi_{s1}+\tilde{\omega}\bar{t})]/(1+\tilde{m})^2, \qquad (38)$$

$$A_{44}=[-2\zeta(1+\tilde{m})+2\zeta\tilde{m}(1+\tilde{m})\cos^2(\phi_{s1}+\tilde{\omega}\bar{t})$$
$$-\tilde{m}(1+\tilde{m})\tilde{\omega}\sin(\phi_{s1}+\tilde{\omega}\bar{t})\cos(\phi_{s1}+\tilde{\omega}\bar{t})$$
$$-\tilde{m}^2(1+\tilde{m})\tilde{\omega}\sin[\phi_{s1}+\tilde{\omega}\bar{t})\cos(\phi_{s1}+\tilde{\omega}\bar{t})]/$$
$$(1+\tilde{m})^2, \qquad (39)$$

$$A_{45}=[\tilde{m}(1+\tilde{m})\tilde{\omega}^2\cos[\phi_{s1}+\tilde{\omega}\bar{t})-\tilde{m}^2(1+\tilde{m})\tilde{\omega}^2$$
$$\cos(\phi_{s1}+\tilde{\omega}\bar{t})]/(1+\tilde{m})^2, \qquad (40)$$

$$A_{46}=[-2\tilde{m}(1+\tilde{m})\tilde{\omega}\sin(\phi_{s1}+\tilde{\omega}\bar{t})-\tilde{m}(1+\tilde{m})^2$$
$$\sin(\phi_{s1}+\tilde{\omega}\bar{t})\cos(\phi_{s1}+\tilde{\omega}\bar{t})$$
$$-\tilde{m}\mathrm{B}'(1+\tilde{m})^2\cos(\phi_{s1}+\tilde{\omega}\bar{t})]/(1+\tilde{m})^2, \qquad (41)$$

$$A_{61}=-\sin(\phi_{s1}+\tilde{\omega}\bar{t}), \qquad (42)$$

$$A_{62}=(1+\tilde{m})\tilde{\omega}\cos(\phi_{s1}+\tilde{\omega}\bar{t})-2\zeta\sin(\phi_{s1}+\tilde{\omega}\bar{t}), \qquad (43)$$

$$A_{63}=\cos(\phi_{s1}+\tilde{\omega}\bar{t}), \qquad (44)$$

$$A_{64}=-(1+\tilde{m})\tilde{\omega}\sin(\phi_{s1}+\tilde{\omega}\bar{t})+2\zeta\cos(\phi_{s1}$$
$$+\tilde{\omega}\bar{t}), \qquad (45)$$

$$A_{65}=-\tilde{m}\tilde{\omega}^2, \qquad (46)$$

$$A_{66}=-(1+\tilde{m})[\mathrm{B}'+\sin(\phi_{s1}+\tilde{\omega}\bar{t})]. \qquad (47)$$

However, in Eq. (27), $\ddot{\tilde{x}}_0$, $\ddot{\tilde{y}}_0$, $\dot{\tilde{x}}_0$, and $\dot{\tilde{y}}_0$ are dropped because these are transient oscillations that disappear with time.

The Floquet theory has been developed for characterizing the functional behavior of linear ordinary differential equations with periodic coefficients. In equation (30), $[A(\bar{t})]$ is an 6 by 6 matrix such that $[A(\bar{t}+T)]=[A(\bar{t})]$ where T is period of the system matrix, $[A(\bar{t})]$. To determine the eigenvalues and hence the characteristic exponents of (29), one can numerically calculate a fundamental set of solutions $[U]$. $[U]$ satisfies the matrix equation (29) of $[\dot{U}]=[A(\bar{t})][U]$ using the initial conditions $[U(0)]=[I]$ during a period of oscillation. Then $[U(T)]$, nonsingular constant 6 by 6 matrix, is obtained as

$$[U(\Delta t)]=[I]+\Delta t[A(0)][U(0)],$$
$$[U(2\Delta t)]=[U(\Delta t)]+\Delta t[A(\Delta t)][U(\Delta t)],$$
$$[U(3\Delta t)]=[U(2\Delta t)]+\Delta t[A(2\Delta t)][U(2\Delta t)],$$

$\cdots\cdots\cdots$, and (48)

$$[U(T)]=[U(T-\Delta t)]+\Delta t[A(T-\Delta t)][U(T-\Delta t)]$$

Solving the characteristic equation, $\|[U(T)]-\mu[I]\|=0$, yields a set of characteristic multipliers, *i. e.* the characteristic roots, μ's, of the matrix $[U(T)]$. To investigate dynamic stability of the Eq. (29), numerical simulation was carried out using the Floquet algorithm. Figures 3 to 8 show the results of computer simulation of the Floquet algorithm when $\tilde{\omega}$ is 1.5 (above critical speed), 1.0 (at critical speed), and 0.7 (below critical speed) with only one ball. The input data were chosen as $\tilde{m}=0.005$, $\zeta=0.01$, and $\phi_{s1}=\pi$. Figure 3 is a plot of the characteristic multipliers, μ's, in complex plane above critical speed ($\tilde{\omega}=1.5$). From this figure the moduli, *i. e.*, absolute values, of the characteristic multipliers are found to be a set of {0.9765, 0.9765, 0.9562, 0.9562, 0.9833, 0.9833} and all of the moduli are less than 1, *i.e.*, all of the moduli are inside of the unit circle. Therefore, the perturbed motion is said to be stable above critical speed when $\beta'=0.01$. Figure 4 is a plot of the characteristic multipliers in complex plane at critical speed ($\tilde{\omega}=1.0$) when $\beta'=0.01$. From this figure the moduli of the characteristic multipliers are found to be a set of {1.302, 1.302, 0.717, 0.717, 0.9238, 0.9508} and two of the moduli (#1 and #2) are greater than 1, *i.e.*, #1 and #2 are outside of the unit circle. Therefore, when $\beta'=0.01$ the perturbed motion is

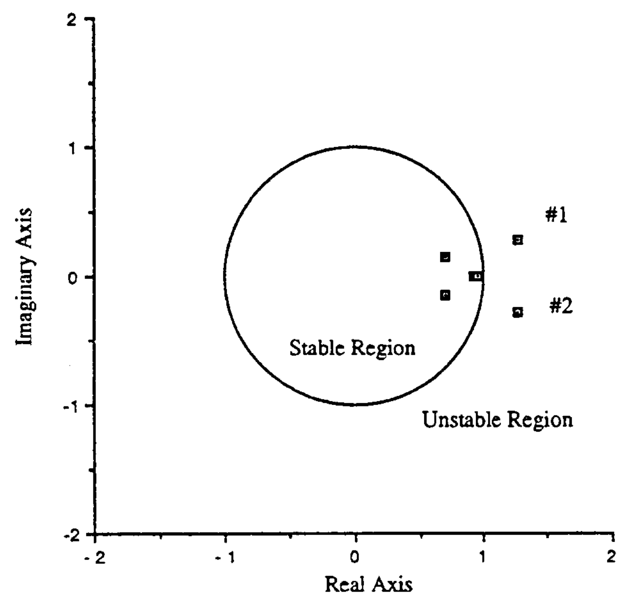

Fig. 4 Characteristic multipliers($\tilde{\omega}=1.0$ and $\beta'=0.01$ case) (Characteristic multipliers: $1.2712\pm0.2814i$, $0.7028\pm0.1435i$, 0.9238, and 0.9508)

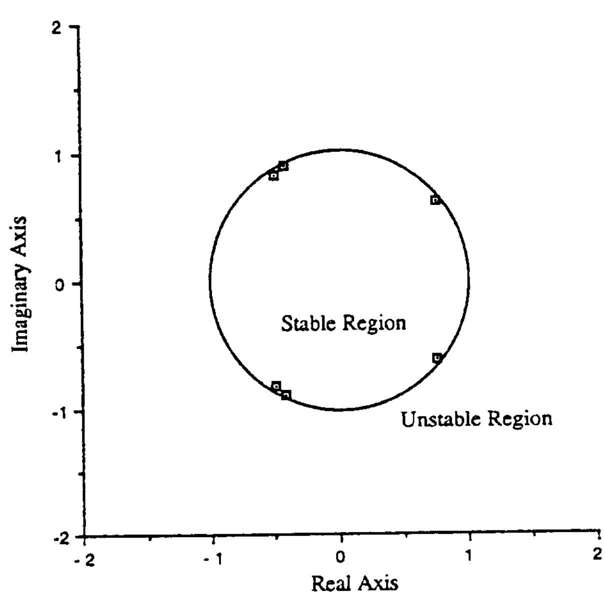

Fig. 3 Characteristic multipliers($\tilde{\omega}=1.5$ and $\beta'=0.01$ case) (Characteristic multipliers: $-0.4129\pm0.8925i$, $0.7617\pm0.6116i$, and $-0.4925\pm0.8197i$)

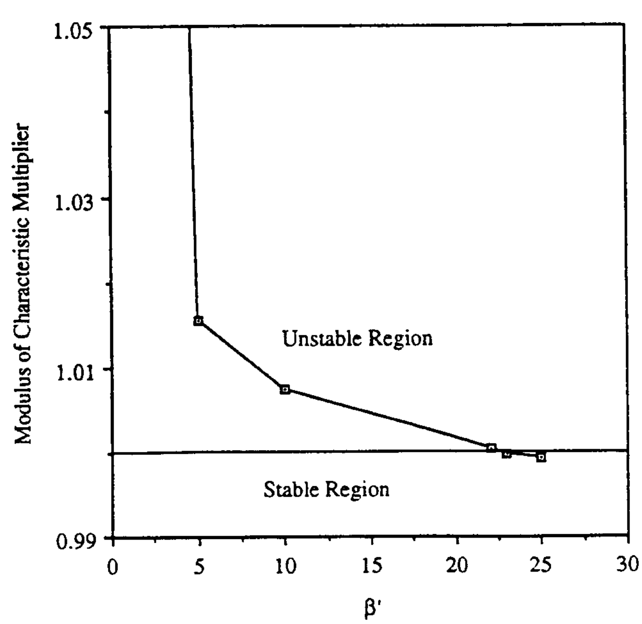

Fig. 5 Modulus of characteristic multiplier versus β'($\tilde{\omega}=1.0$ case)

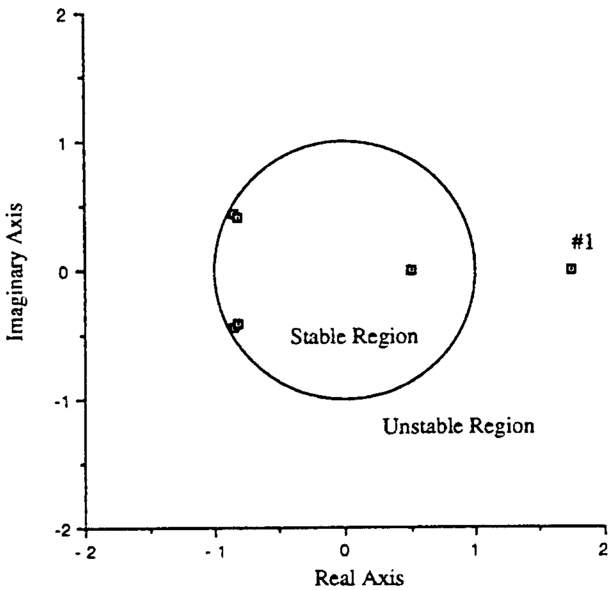

Fig. 6 Characteristic multipliers($\tilde{\omega}\doteq0.7$ and $\beta'=0.01$ case) (Characteristic multipliers: 1.7514, 0.5059, $-0.8181\pm0.4060i$, and $-0.8517\pm0.4446i$)

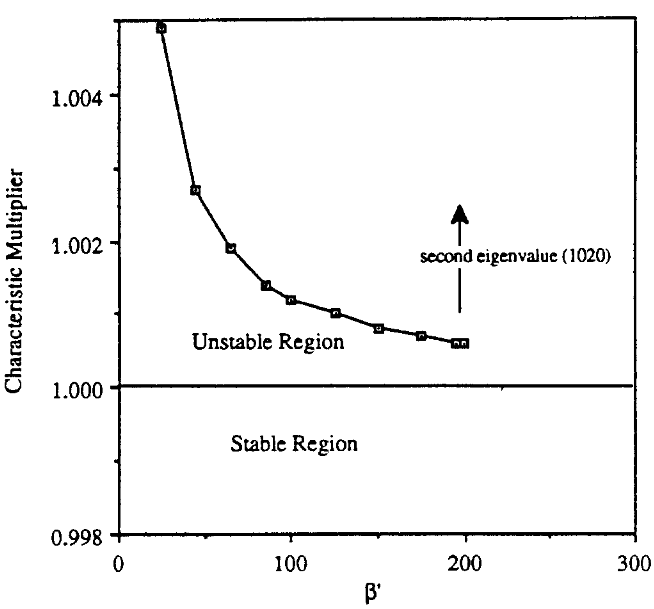

Fig. 7 Modulus of characteristic multiplier versus β'($\tilde{\omega}=0.9$ case)

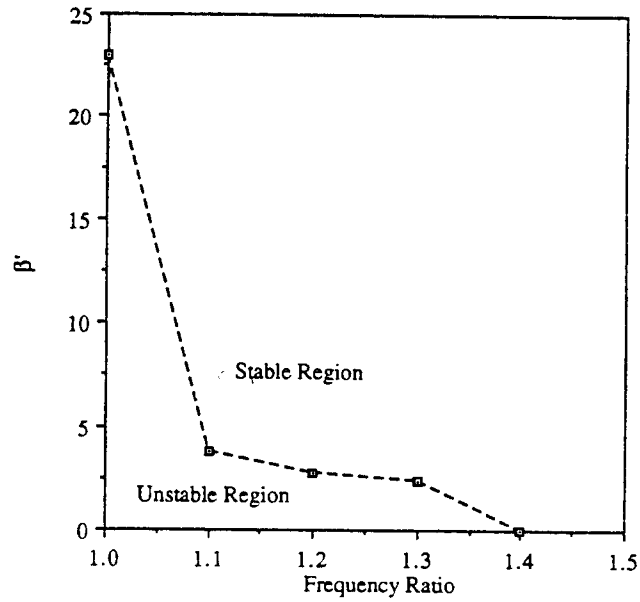

Fig. 8 Dynamic stability diagram($\tilde{\omega}$ versus β')

unstable at critical speed. Figure 5 is a plot of one of the moduli of the characteristic multipliers versus β' at critical speed ($\tilde{\omega}=1.0$). However, From this figure increased β' can yield a stable system at critical speed. Figure 6 is a plot of the characteristic multipliers in complex plane below critical speed ($\tilde{\omega}<1$) when $\beta'=0.01$. From this figure the moduli of the characteristic multipliers are given by the set {1.7514, 0.5059, 0.9133, 0.9133, 0.9607, 0.9607} and one of the moduli (#1) is greater than 1, i.e., #1 is outside of the unit circle and the system is unstable. Figure 7 is a plot of one of the characteristic multipliers versus β' below critical speed ($\tilde{\omega}=0.9$). From this figure increased β' does not appear to be able to make the system stable below critical speed. Therefore, the perturbed motion appears to be unstable below critical speed. Figure 8 shows a dynamic stability diagram of the perturbed motion (β' versus $\tilde{\omega}$). From this diagram the damping coefficient, β', of the fluid plays an important role in the stability of the perturbed motion.

6. Conclusions

Many inventors have suggested various kinds of Self-Compensating Dynamic Balancer through U.S. patents, but they left it for others to explain why this system will work or will not work with solid balls and damping fluid which has a low viscosity. To the author's knowledge, the motion analysis of the balls and the rotating shaft as presented in this paper represents the first attempt to analyze the dynamic stability of an SCDB with solid balls and damping fluid.

From the preceding work, the following conclusions were drawn. The equations of motion of the balls were derived by the Lagrangian method. Steady solutions were derived from the analytic model. Perturbation solutions were also obtained from the analytic model. To investigate dynamic stability of the perturbed motion numerical simulation of the Floquet algorithm with only one ball was conducted. Based on the results of stability investigation, ball positions that result in a balanced system are stable above the critical speed for $\beta' \geqq 3.8$. At critical speed the perturbed motion is said to be stable for $\beta' = 23$. However, the system appears to be unstable below critical speed. However, further study of this Self-Compensating Dynamic Balancer for a nonuniform rotating system with variable rotating speed and the effect of β' on dynamic stability for multiple balls should be done in the future.

References

(1) Darlow, M.S., 1989, Balancing of High-Speed Machinery, Springer-Verlag, New York.

(2) Rieger, N.F., 1986, Balancing of Rigid and Flexible Rotors, The Shock and Vibration Information Center, U.S. Department of Defense.

(3) Nayfeh, A.H. and Mook, D.T., 1979, Nonlinear Oscillations, John Wiley & Sons, New York.

(4) Hahn, W., 1967, Stability of Motion, Springer-Verlag, New York.

(5) Hayashi, C., 1964, Nonlinear Oscillations in Physical Systems, Princeton University Press.

(6) Thearle, E.L. and Schenectady, N.Y., 1934, "Dynamic Balancing of Rotating Machinery in the Field," Journal of Applied Mechanics, APM-56-19, pp. 745-753.

(7) Akimoff, N.W., 1917, "Recent Developments in Balancing Apparatus," The Journal of the ASME, Vol. 39, pp. 987-990.

(8) Baker, J.G., 1939, "Mathematical-Machine Determination of the Vibration of Accelerated Unbalanced Rotor," Journal of Applied Mechanics, Vol. 61, pp. A-145-A-150.

(9) Kroon, R.P., 1943, "Balancing of Rotating Apparatus-I," Journal of Applied Mechanics, Vol. 65, pp. A-225-A-228.

(10) Kroon, R.P., 1944, "Balancing of Rotating Apparatus-II," Journal of Applied Mechanics, Vol. 66, pp. A-47-A-50.

(11) Church, A.H. and Plunkett, R., 1961, "Balancing Flexible Rotors," Journal of Engineering for Industry, pp. 383-389.